

Finite-duration seeding effects in powerful backward Raman amplifiers

N. A. Yampolsky, V. M. Malkin, and N. J. Fisch

Department of Astrophysical Sciences, Princeton University, Princeton, New Jersey 08544, USA

(Received 1 July 2003; published 11 March 2004)

In the process of backward Raman amplification (BRA), the leading layers of the seed laser pulse can shadow the rear layers, thus weakening the effective seeding power and affecting parameters of output pulses in BRA. We study this effect numerically and also analytically by approximating the pumped pulse by the “ π -pulse” manifold (family) of self-similar solutions. We determine how the pumped pulse projection moves within the π -pulse manifold, and describe quantitatively the effective seeding power evolution. Our results extend the quantitative theory of BRA to regimes where the effective seeding power varies substantially during the amplification. These results might be of broader interest, since the basic equations are general equations for resonant three-wave interactions.

DOI: 10.1103/PhysRevE.69.036401

PACS number(s): 52.38.Bv, 52.35.Mw, 42.65.Yj, 42.65.Dr

I. INTRODUCTION

Backward Raman amplification might be utilized to achieve ultrahigh laser powers [1]. In this scheme, a short pumped pulse consumes essentially all of a long incident pump power through the resonant stimulated backward Raman scattering in plasma. The pulse also contracts as its amplitude grows. The amplification is fast enough to reach nearly relativistic pumped pulse intensities, within times shorter than it takes for filamentation instabilities to develop. By nearly relativistic intensities we mean those intensities for which the electron motion in the pulse fields becomes nearly relativistic, that is 10^{17} W/cm² for $\lambda=1\text{-}\mu\text{m}$ -wavelength radiation. Such a nonfocused intensity would be 10^5 times higher than what is currently available through the chirp pulse amplification technique [2]. The focused intensities would be 10^{25} W/cm² for a $\lambda=1\text{-}\mu\text{m}$ -wavelength output pulse focused from 10-cm to 10- μm diameter. For shorter wavelength lasers, the electron motion becomes relativistic only at higher intensities, so achievable nonfocused and focused intensities could be even higher yet [1,3].

The optical system of backward Raman amplifiers naturally separates into two components: a pump block consisting of one or several laser beams delivering large powers with low requirements on optical precision, and a seed block delivering a higher precision, lower power short laser pulse to extract and focus the pump energy [1,4]. The output pulses should maintain a high focusability of relatively low intensity input seeds even in the presence of plasma noise [5] and substantial pump fluctuations [6], including the possibility of multiple pumps [7].

In this paper, we show how the output pulse depends upon the short duration of the input seed pulse. To develop the terminology for expressing this dependence, consider how the amplification mechanism operates: Upon the arrival of the short seed pulse to any given layer of plasma, the pump and seed pulses resonantly interact to generate a fresh Langmuir wave. The short seed quickly leaves this plasma layer and proceeds to interact with a fresh pump and fresh plasma, hardly being affected by the interaction. Meanwhile, the Langmuir wave stays at the plasma layer, where it continues to backscatter the pump, thereby growing further. The back-

scattered light, growing after the original seed has passed, we call “the pumped pulse.” It has the same frequency as the seed pulse and propagates in the same direction, trailing the seed. It can grow to intensities much greater than the original seed until the pump is depleted, and then can further grow (and contract) even to intensities much greater than the pump.

Note that the backward Raman amplification along each ray is essentially a one-dimensional process. As long as effects of the input seed pulse finite duration can be neglected, the pumped pulse evolution approaches, at an advance nonlinear stage, a self-similar regime known as the “ π -pulse” regime [8,1,3]. The π -pulse amplitude grows linearly with the amplification distance while the π -pulse duration decreases inversely with the amplitude. There is a family of such self-similar solutions that can be conveniently characterized by the location z_s of the (physically of zero duration) seed and the location z_M of the pumped pulse intensity maximum. This maximum propagates behind the original seed, approaching it as the pumped pulse grows and contracts. When the pumped pulse duration becomes comparable to the original seed duration, the pumping that arises from the rear layers of the original seed becomes noticeably less than that arising from the front layers. The rear layers of the original seed are then noticeably shadowed by pumping arising from the leading layers and causing the pump depletion. This reduces the area of the original seed, which effectively contributes to the amplification.

We define an effective dimensionless area under the seed pulse envelope ϵ_{eff} , which can be called an “effective seeding power.” It can be expressed in terms of the parameters z_s and z_M , i.e., locations of the effective seed and the pumped pulses maxima. For small $\epsilon_{\text{eff}} \ll 1$, the π -pulse maximum location depends on ϵ_{eff} logarithmically. Thus, changing ϵ_{eff} , say, by a factor of 2 does not noticeably affect the pumped pulse, which remains close to the π -pulse manifold. This enables us to describe the actual pulse evolution in terms of the matching π -pulse evolution within the π -pulse manifold.

The major goal of this paper is to define the matching π -pulse parameters and to describe their evolution. This will enable us to extend quantitatively the theory of backward

Raman amplification to regimes where the effective seeding power varies substantially during the amplification.

The paper is arranged as follows. First, we show numerically that, throughout the entire advanced nonlinear stage of the amplification, the pumped pulse indeed can be very well approximated by a pulse growing from a seed of a negligibly short duration and varying effective seeding power ϵ_{eff} (Sec. III). Then, we analytically describe (Secs. IV and V), the motion of the pumped pulse projection within this special manifold of pulses growing from negligibly short seeds.

II. BASIC EQUATIONS AND π -PULSE MANIFOLD

Resonant Raman backscattering in a plasma can be described by the following equations for the wave envelopes (see, for instance, Refs. [10,3]):

$$a_t + ca_z = -\omega_p f b, \quad b_t - cb_z = \omega_p a f^*, \quad f_t = \omega b^*/2, \quad (1)$$

where ω_p is the electron plasma frequency, $\omega \gg \omega_p$ is the pump laser frequency, a and b are the dimensionless space-time envelopes of the pump and pumped pulse electric field amplitudes, respectively, normalized so that the pump intensity (i.e., power density) is $I_a = \pi c (m_e c^2 / e)^2 |a|^2 / \lambda^2 = 2.736 \times 10^{18} |a|^2 / \lambda^2 [\mu\text{m}] \text{ W/cm}^2$, with a similar normalization for the seed b , while f is an appropriately normalized Langmuir wave envelope; λ is the laser wavelength, t is the time, z is the distance in the direction of the pump propagation, subscripts denote the respective derivatives, and c is the vacuum speed of light. The pumped laser frequency is downshifted by ω_p from the pump frequency; the laser wave numbers are close to ω/c and the resonant Langmuir wave-number is close to $2\omega/c$. The slowly varying envelope approximation (1) is applicable as long as the characteristic space and time scales of the wave envelopes substantially exceed $c\omega_p^{-1}$ and ω_p^{-1} , respectively. We also assume conditions are satisfied that allow one to neglect the effects of dispersion, diffraction, wave breaking, self-focusing, and self-phase-modulation and generation of other harmonics.

For further analysis, it is convenient to rewrite equations (1) in the variables

$$\zeta = (t + z/c) \sqrt{\omega\omega_p}/2, \quad \tau = -z \sqrt{\omega\omega_p}/c, \quad f = \bar{f} \sqrt{\omega/\omega_p},$$

thus getting

$$a_\zeta - a_\tau = -\bar{f} b, \quad b_\tau = a \bar{f}^*, \quad \bar{f}_\zeta = a b^*. \quad (2)$$

During the linear stage of the backscattering instability, when the pump depletion is negligible, so that $a \approx a_0 = \text{const}$, the solution of Eqs. (2) is given by the formulas (Refs. [11,3])

$$b(\zeta, \tau) = \frac{\partial}{\partial \zeta} \int d\zeta_1 G(\zeta - \zeta_1, \tau) b(\zeta_1, 0), \quad (3)$$

$$G(\zeta, \tau) = I_0(2\sqrt{\eta}), \quad \eta = a_0^2 \zeta \tau = \xi^2/4, \quad (4)$$

where I_0 is the modified zero-order Bessel function.

During an advanced nonlinear stage of the instability, when the pumped pulse amplification length is much larger than the pulse duration (within which it completely depletes the pump), the term a_τ in Eqs. (2) can be neglected compared to the term a_ζ . Thus simplified, Eqs. (2) conserve the joint density of the pump photons and Langmuir plasmons:

$$\frac{\partial}{\partial \zeta} (|a|^2 + |\bar{f}|^2) = 0. \quad (5)$$

Real solutions can be then searched for in the form

$$a(\zeta, \tau) = a_0 \cos(u/2), \quad \bar{f}(\zeta, \tau) = a_0 \sin(u/2), \quad (6)$$

$$b(\zeta, \tau) = u_\zeta/2, \quad (7)$$

which reduces the set to the sine-Gordon equation

$$u_{\zeta\tau} = a_0^2 \sin u. \quad (8)$$

This sine-Gordon equation has a special set of self-similar solutions $u(\zeta, \tau) = U(\xi \equiv 2a_0 \sqrt{\zeta\tau})$ satisfying the equation

$$U_{\xi\xi} + U_\xi/\xi = \sin U, \quad U(+0) = \epsilon, \quad (9)$$

and depending on the single parameter ϵ . This is the classical π -pulse attractor solution (Ref. [8]) that is established at the advanced nonlinear stage of the backward Roman amplification (BRA) for seeds of a negligibly short duration.

Note that, for the π -pulse solution, the relative value of the neglected term a_τ in the energy-containing domain is about $\xi_M/a_0^2 \tau^2$ (where ξ_M is the location of the π -pulse maximum in a self-similar variable ξ), which indeed quickly decreases as the amplification proceeds.

III. VARYING EFFECTIVE SEEDING POWER FOR SEEDS OF FINITE DURATION

As noted above, the shadowing of rear layers of the seed pulse can affect the actual BRA. For a zero-duration seed $b(z=0, t) = \epsilon \delta(t) / \sqrt{\omega\omega_p} = \epsilon \delta(\zeta) / 2$, formally considered within Eqs. (1) or (2), the shadowing effect is absent and the seeding power, constant throughout the amplification length, can be defined as the dimensionless area under the seed envelope $\epsilon = 2 \int b(\tau=0, \zeta) d\zeta$. Such zero-duration seed solutions tend asymptotically, at large amplification lengths $-z$, to the π -pulse manifold.

To define precisely the effective seeding power ϵ_{eff} for seeds of finite duration, we formally match the real pumped pulse with the pulse growing from a zero-duration seed and reaching the same maximum pumped amplitude within the same amplification length $-z$ for the same pump amplitude a_0 . The ‘‘same amplification length’’ here is the length traversed by the original seed pulse maximum. Note that the pumped pulse maximum (trailing the original seed pulse) does not then coincide with the maximum of the pulse growing from a zero-duration seed; the maxima are separated by a distance which we define as z_0 .

Figure 1 shows a numerical example of the effective seeding power ϵ_{eff} for the Gaussian seed $b(z=0, t) = \epsilon$

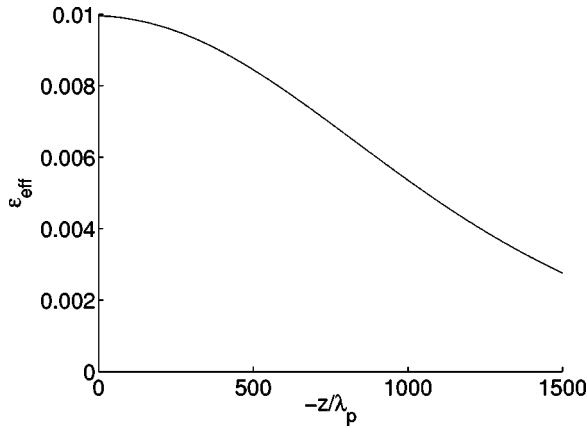


FIG. 1. Varying effective seeding power ϵ_{eff} for the Gaussian seed pulse of duration $T=2\pi/\omega_p$ in BRA.

$\times \exp[-(t/T)^2]/T\sqrt{\omega\omega_p\pi}$, with $T=2\pi/\omega_p$, $\epsilon=0.01$, $\lambda_p=2\pi c/\omega_p=12\ \mu\text{m}$, $\lambda=1\ \mu\text{m}$ and $a_0=0.006$.

Figure 2 shows the shift z_0 between the locations of amplitude maximum for the actual pumped pulse and the matching pumped pulse growing from a zero-duration seed, for the same numerical example as above.

To compare shapes of the real and matching pumped pulses (growing from a finite- and zero-duration seeds, respectively) in the above numerical example, we shift the zero-duration seed by z_0 , thus matching the locations of maxima for the pumped pulses. Figure 3 indicates that the pulse envelopes indeed coincide very well even for noticeable variations of ϵ_{eff} .

In Fig. 3, larger rescaled amplitude maxima correspond to larger values of ϵ_{eff} , i.e., to smaller amplification lengths. The apparent drift of the pumped pulse amplitude maximum to larger η in the upper plots (taking place just in the self-similar variable η) attests to the fact that the leading spike of the self-similar (π -pulse) solution is further from its zero-duration seed (located at $\eta=0$ in these plots) for smaller ϵ_{eff} . In physical variables z and t , the leading spike moving with a superluminal velocity approaches the zero-duration seed all the time. In lower plots of Fig. 3, placing the Gaussian seed

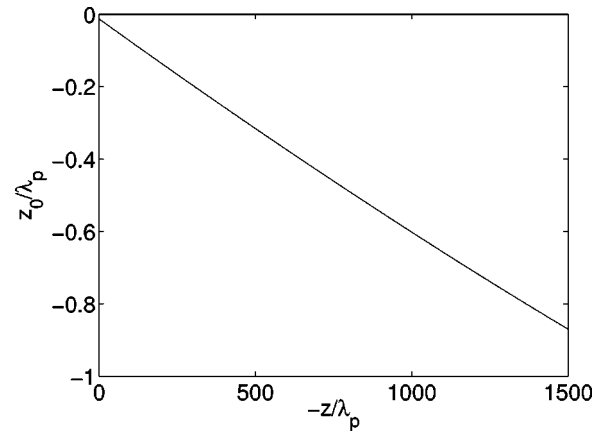


FIG. 2. Varying shift z_0 between the amplitude maxima of the real and matching pumped pulses (growing from the Gaussian seed pulse of duration $T=2\pi/\omega_p$ and zero-duration seed, respectively).

maximum at $\eta=0$, the pumped seed maximum approaches the origin even in self-similar variables. This occurs because, in the process of amplification, the major seeding comes from more and more advanced leading layers of the Gaussian seed.

Note that using a longer seed would result in an earlier decrease of ϵ_{eff} . Seeds longer than the Raman length $c/(a_0\sqrt{\omega\omega_p/2})$ would in fact use just their leading Raman-length-long part right away during the linear stage of the amplification. Also note, that short Gaussian seeds, like one used above, are favorable for eliminating deleterious superluminal precursors (Ref. [9]).

IV. SINE-GORDON APPROXIMATION

As seen from the derivation of the sine-Gordon equation, it can well approximate real solutions of the original equations (1) or (2) at the advanced nonlinear stage of the pulse amplification when the term a_τ in Eq. (2) can be neglected, and also during the linear stage of the pulse amplification when the pump variation can be entirely neglected. Thus, there is just a relatively short early nonlinear stage of the

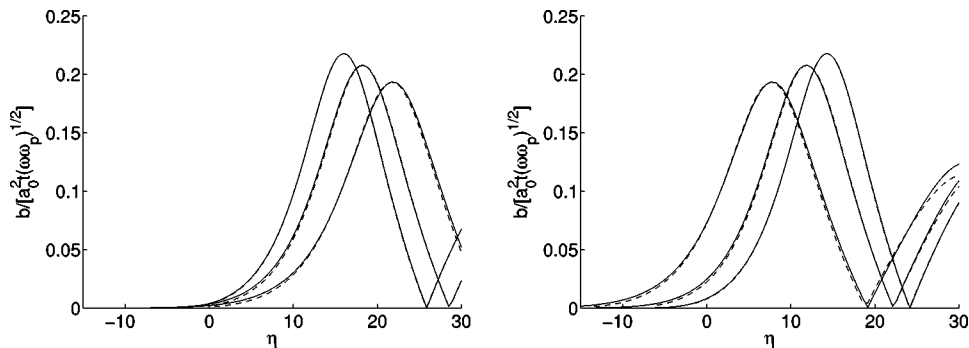


FIG. 3. Rescaled amplitude for the pumped pulse growing from the Gaussian seed pulse of duration $T=2\pi/\omega_p$ (solid lines) and the matching pumped pulse growing from the zero-duration seed (dashed lines) vs $\eta=a_0^2\zeta\tau=a_0^2\omega\omega_p(t+z/c)(-z/c)/2$ at the amplification lengths $-z/\lambda_p=500, 1000, \text{ and } 1500$ ($\lambda_p=2\pi c/\omega_p$). Larger rescaled amplitude maxima correspond to larger values of ϵ_{eff} , i.e., to smaller amplification lengths. In the left plot, the matching zero-duration seed is located at $\eta=0$, while in the right plot, the Gaussian seed maximum is located at $\eta=0$.

pulse amplification when the sine-Gordon approximation might not be applicable.

The amplification length around which the complete pump depletion occurs for the first time can be evaluated as follows. During the linear stage, the integrated amplitude u of the pumped pulse can be presented, according to Eqs. (3) and (7), in the form

$$u_{lin}(\zeta, \tau) = 2 \int d\zeta_1 G(\zeta - \zeta_1, \tau) b(\zeta_1, 0), \quad (10)$$

which gives, for a seed much shorter than the Raman length,

$$u_{lin}(\zeta, \tau) \approx \epsilon I_0(2a_0 \sqrt{\zeta \tau}) \equiv \epsilon I_0(\xi). \quad (11)$$

For a given t , the product $\zeta \tau$ has a maximum at $z = -ct/2$, so that the maximum of the integrated amplitude u moves with the speed $-c/2$ during the linear amplification stage. For a small enough $\epsilon \ll 1$, the pumped pulse makes many exponentiations before reaching the nonlinear stage, which allows one to use the asymptotic formula $I_0(\xi) \approx e^\xi / \sqrt{2\pi\xi}$ at $\xi \gg 1$ for an advanced linear stage of the pulse amplification. The same condition allows one to approximate the leading pumped spike in the nonlinear pump depletion regime by the classical 2π -pulse solution of the sine-Gordon equation. Then, both the linear front and the maximum domains of the leading pumped spike can be described by a single formula (Ref. [1])

$$u \approx 4 \arctg[\epsilon I_0(\xi)/4] \approx 4 \arctg(u_{lin}/4). \quad (12)$$

The condition for the pump complete depletion $u \approx \pi$ then reads as $\epsilon I_0(\xi) \approx 4$, thus defining the value $\xi = \xi_*$ at which the depletion occurs. This takes place for the first time near the location

$$-z_* \approx ct_*/2 \approx c \xi_* / a_0 \sqrt{2\omega\omega_p}. \quad (13)$$

A numerical comparison of solutions of the original equation and the sine-Gordon equation indicates that the sine-Gordon solution does not depart much from the original solution even during the early nonlinear stage of the pulse amplification, as illustrated by Fig. 4.

Thus, the sine-Gordon approximation appears to be reasonably accurate throughout the entire amplification process. As noted above, the π -pulse manifold is the family of self-similar solutions of the sine-Gordon equation. These solutions correspond to zero-duration seed initial conditions $u(\zeta, \tau=0) = \epsilon \Theta(\zeta - \zeta_s)$, where $\Theta(\zeta) = 1$ for $\zeta > 0$ and $\Theta(\zeta) = 0$ for $\zeta < 0$ is the unit step function. It follows that the π -pulse manifold can also approximate well the entire amplification process. Indeed, the linear and even early nonlinear stages can be approximated by the domain $\xi \leq \xi_*$ of the π -pulse, as explained earlier in this section. At advanced nonlinear stage, the π -pulse is known to be an attractor solution for all ξ .

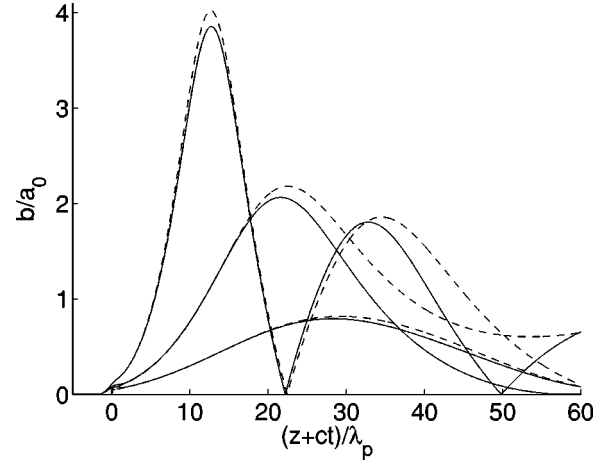


FIG. 4. Sine-Gordon approximation (dashed lines) to the pumped pulse amplitude (solid lines) calculated from the original equations (1) at $t\omega_p/2\pi = 75, 100,$ and 150 as a function of $(z + ct)/\lambda_p$. The seed and pump are the same as above: $a_0 = 0.006$, $\lambda = 1 \mu\text{m}$, $\lambda_p = 12 \mu\text{m}$, $b(z=0, t) = \epsilon \exp(-t^2/T^2)/T \sqrt{\omega\omega_p \pi}$, $T = 2\pi/\omega_p$, and $\epsilon = 0.01$. The pump complete depletion occurs for the first time at $t\omega_p/2\pi \approx 100$ which agrees with formula (13).

V. ANALYTICAL APPROXIMATION

The pump amplitude a_0 can be excluded from the sine-Gordon equation (8) by a simple rescaling of independent variable $\bar{\tau} = a_0^2 \tau$. Up to this rescaling, there is a two-dimensional π -pulse manifold to approximate solutions growing from short yet finite-duration seeds. In this section we derive simple analytical formulas describing dynamics of such solutions projected on the π -pulse manifold, namely, evolution of the matching zero-duration seed and pumped pulse maximum locations ζ_0 and ζ_M .

The leading layers of the pumped pulse can be described by the linear theory formula (10). This description can be extended to the nonlinear domain of the leading spike through approximating it, to zeroth order, by the 2π -pulse, $u \approx 4 \arctg(u_{lin}/4)$. Location of the 2π -pulse maximum can be determined from the equation $u \approx \pi \Rightarrow u_{lin} \approx 4$. The respective $\zeta = \zeta_M$ satisfies then the equation

$$\int d\zeta_1 I_0[2\sqrt{(\zeta_M - \zeta_1)\bar{\tau}}] b(\zeta_1, 0) \approx 2. \quad (14)$$

The integrated function varies rapidly in ζ_1 , so that the major contribution to the integral comes from a narrow vicinity of this function maximum $\zeta_1 = \zeta_{01}$. Expanding the logarithm function near the maximum,

$$S \equiv \ln\{I_0[2\sqrt{(\zeta_M - \zeta_1)\bar{\tau}}] b(\zeta_1, 0)\} \approx S_0 - S_2(\zeta_1 - \zeta_{01})^2, \quad (15)$$

one can present Eq. (14) in the simplified form

$$I_0[2\sqrt{(\zeta_M - \zeta_{01})\bar{\tau}}] b(\zeta_{01}, 0) \sqrt{\pi/S_2} \approx 2. \quad (16)$$

Equation (16), together with the function S maximum condition,

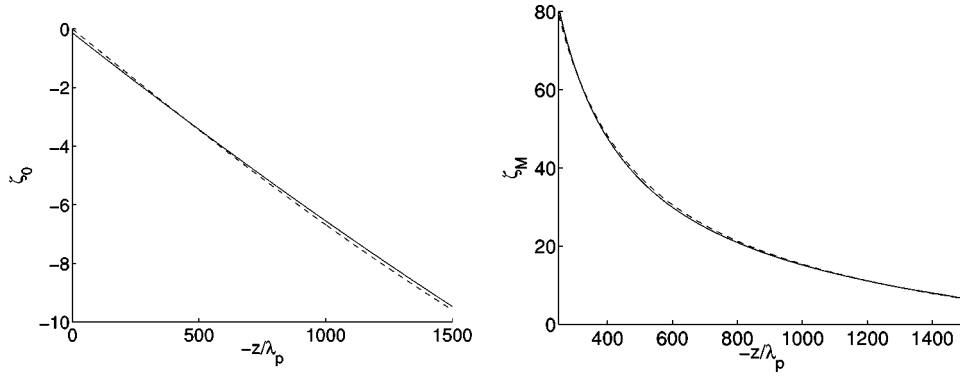


FIG. 5. Locations of the matching zero-duration seed ζ_0 (left figure) and the pumped pulse maximum (in ζ at fixed τ or z) ζ_M (right figure) as functions of the amplification length $-z$, found numerically as in Sec. III (solid lines) and analytically (dashed lines).

$$\frac{\partial}{\partial \zeta_{01}} \ln \{ I_0 [2 \sqrt{(\zeta_M - \zeta_{01}) \bar{\tau}}] b(\zeta_{01}, 0) \} = 0, \quad (17)$$

and the definition

$$S_2 = - \frac{\partial^2}{2 \partial \zeta_{01}^2} \ln \{ I_0 [2 \sqrt{(\zeta_M - \zeta_{01}) \bar{\tau}}] b(\zeta_{01}, 0) \}, \quad (18)$$

define the $\bar{\tau}$ -dependent location of the pumped pulse maximum ζ_M together with the auxiliary parameter ζ_{01} . For known ζ_M , the effective seed location ζ_0 is determined as ζ_0 maximizing the product of the nonlinear amplification factor $N(\zeta_M - \zeta_0)$ and the actual seed amplitude $b(\zeta_0)$. It is convenient to present the maximum condition in the form

$$\frac{\partial}{\partial \zeta_0} \ln [N(\zeta_M - \zeta_0) b(\zeta_0, 0)] = 0. \quad (19)$$

The log slope of nonlinear amplification factor $N(\zeta_M - \zeta_0)$ can be evaluated, in the above 2π -pulse approximation $u_{lin}/4 \approx \text{tg}(u/4)$ at $u = \pi \Rightarrow u_{lin} \approx 4$, as

$$\frac{\partial \ln u}{\partial \zeta} \approx \frac{2}{\pi} \frac{\partial \ln u_{lin}}{\partial \zeta}.$$

It follows that,

$$\frac{2}{\pi} \frac{\partial}{\partial \zeta_0} \ln \{ I_0 [2 \sqrt{(\zeta_M - \zeta_0) \bar{\tau}}] \} + \frac{d}{d\zeta_0} \ln b(\zeta_0, 0) = 0. \quad (20)$$

This determines the effective seed location ζ_0 . A numerical example is presented in Figs. 5 and 6.

Figure 5 compares thus calculated parameters ζ_0 and ζ_M of the matching π -pulse and the numerically calculated (as described in Sec. III) respective parameters of the actual pumped pulse growing from the same (as in previous sections) Gaussian seed $b(z=0, t) = \epsilon \exp(-t^2/T^2)/T \sqrt{\omega \omega_p} \pi \equiv \epsilon \exp(-\zeta^2/\Delta^2)/2\Delta \sqrt{\pi}$ of the duration $\Delta = T \sqrt{\omega \omega_p}/2 = \pi \sqrt{\omega/\omega_p}$. Plots for ζ_M are shown just for an advanced nonlinear amplification stage, because, during the linear

stage, the pumped pulse amplitude is a monotonically increasing function of ζ at fixed τ , which is not the case addressed by the analytical theory considered here.

Figure 6 compares amplitudes of the matching π -pulse with analytically calculated ζ_0 and ζ_M (dashed lines) and of the actual pumped pulse growing from the above Gaussian seed (solid lines). The dotted lines show π -pulses with ζ_0 and ζ_M numerically determined from the actual pumped pulse, as described in Sec. III. The very good coincidence of dotted and dashed lines indicates that their small deviation from solid line at larger $-z$ is not caused by an inaccuracy in calculated ζ_0 and ζ_M .

Note that using asymptotic formula $I_0(\xi) \approx e^\xi / \sqrt{2\pi\xi}$ at $\xi \gg 1$, one could present the equations for calculating parameters ζ_M and ζ_0 of the π -pulse matching the pumped pulse growing from the above Gaussian seed in the following forms:

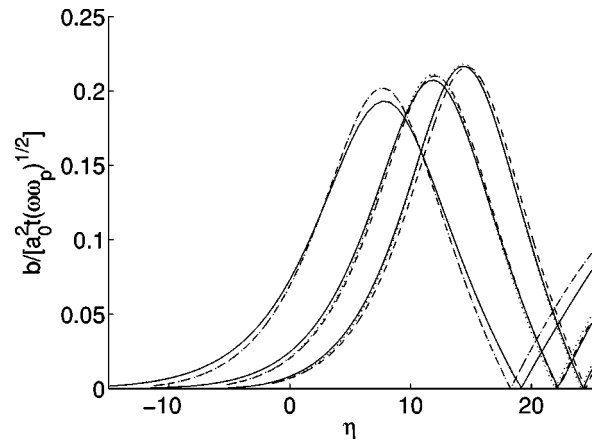


FIG. 6. Normalized amplitude of the actual pumped pulse growing from the Gaussian seed (solid lines), the π -pulse with analytically calculated ζ_0 and ζ_M (dashed lines), and the π -pulse with ζ_0 and ζ_M numerically determined from the actual pumped pulse, as described in Sec. III (dotted lines), for the amplification lengths $-z/\lambda_p = 500, 1000, \text{ and } 1500$. Larger maximum amplitudes correspond to larger values of ϵ_{eff} , i.e., to smaller amplification lengths. The Gaussian seed maximum is located at $\eta=0$.

$$\zeta_{01} \approx -\frac{\Delta^2 \bar{\tau}}{\xi_{M1}} \left(1 - \frac{1}{2\xi_{M1}}\right),$$

$$\xi_{M1} \equiv 2\sqrt{(\zeta_M - \zeta_{01})\bar{\tau}}$$

$$\approx \ln \left[\frac{4}{\epsilon} \sqrt{2\pi \left(\xi_{M1} + \frac{2\Delta^2 \bar{\tau}^2 (1 + \xi_{M1}^{-1})}{\xi_{M1}^2} \right)} \right] + \frac{\zeta_{01}^2}{\Delta^2}, \quad (21)$$

$$\zeta_0 \approx -\frac{2}{\pi} \frac{\Delta^2 \bar{\tau}}{\xi_M} \left(1 - \frac{1}{2\xi_M}\right),$$

$$\xi_M \equiv 2\sqrt{(\zeta_M - \zeta_0)\bar{\tau}}.$$

The lines plotted according to these formulas are nondistinguishable from the dashed lines in Figs. 5.

The approximation of slowly varying π -pulse parameters is justified as long as the pulse maximum location in a self-similar variable ξ_M does not change much within the amplification length:

$$\left| \frac{\partial \ln \xi_M}{\partial \ln \tau} \right| \ll 1. \quad (22)$$

This condition is satisfied for $\Delta^2 \bar{\tau}^2 / \xi_M^3 \ll 1$. Note that, at $\bar{\tau} \rightarrow \infty$, the above equations would formally give

$$\xi_{M1} \approx (\Delta \bar{\tau})^{2/3}, \quad -\zeta_{01} \approx \Delta^{4/3} \bar{\tau}^{1/3}, \quad -\zeta_M \approx 3\Delta^{4/3} \bar{\tau}^{1/3}/4,$$

$$\xi_M \approx 0.72(\Delta \bar{\tau})^{2/3}, \quad -\zeta_0 \approx 0.88\Delta^{4/3} \bar{\tau}^{1/3}.$$

Then, $|\partial \ln \xi_M / \partial \ln \tau| \approx 2/3$, not satisfying Eq. (22), while $\Delta^2 \bar{\tau}^2 / \xi_M^3 \approx 2.68$. In our calculations, the parameter $\Delta^2 \bar{\tau}^2 / \xi_M^3$ reaches the value ≈ 0.25 at $-z = 1500\lambda_p$. It still satisfies Eq. (22), but approaching to this applicability limit causes a small deviation between theoretical and actual pulses, seen in Fig. 6.

The deviation is even more manifest in the effective seeding power ϵ_{eff} that can be calculated from the known $\zeta_M - \zeta_0$. Within the above asymptotic approximation,

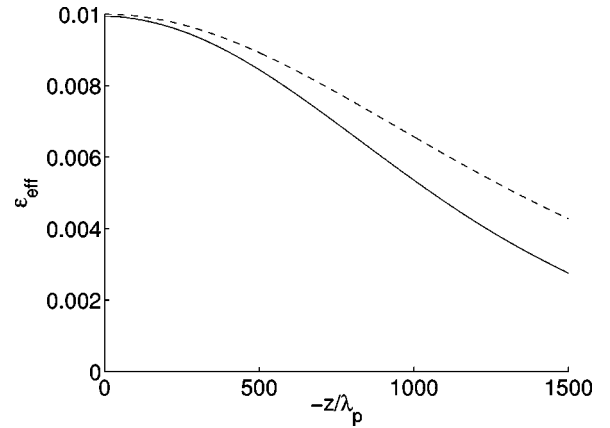


FIG. 7. The effective seeding power ϵ_{eff} calculated numerically, as in Sec. III (solid line), and analytically (dashed line).

$$\epsilon_{\text{eff}} \approx 4\sqrt{2\pi\xi_M} e^{-\xi_M}. \quad (23)$$

Figure 7 compares this theoretical effective seeding power ϵ_{eff} with that numerically calculated as in Sec. III.

VI. CONCLUSION

We have quantitatively described the effect of shadowing the rear layers of short laser seeds by the seed leading layers in powerful backward Raman amplifiers (BRAs). We have shown that such a shadowing results in the pumped pulse sliding along the manifold of self-similar (π -pulse) solutions corresponding to seeds of negligible duration, and derived formulas for parameters of BRA output pulses, taking this sliding into account. Apart from the practical importance of a precise calculation of BRA output pulses, our results are of interest for the general theory of resonant three-wave interactions.

ACKNOWLEDGMENTS

This work was supported by DOE DEFY03098UP00210, DOE DEAC02CH03073, and DARPA.

-
- [1] V.M. Malkin, G. Shvets, and N.J. Fisch, *Phys. Rev. Lett.* **82**, 4448 (1999).
 - [2] G.A. Mourou, C.P.J. Barty, and M.D. Perry, *Phys. Today* **51** (1), 22 (1998); M.D. Perry *et al.*, *Opt. Lett.* **24**, 160 (1999).
 - [3] V.M. Malkin, G. Shvets, and N.J. Fisch, *Phys. Plasmas* **7**, 2232 (2000).
 - [4] N.J. Fisch and V.M. Malkin, *Phys. Plasmas* **10**, 2056 (2003).
 - [5] A. Solodov, V.M. Malkin, and N.J. Fisch, *Phys. Plasmas* **10**, 2540 (2003).
 - [6] G.M. Fraiman, N.A. Yampolsky, V.M. Malkin, and N.J. Fisch, *Phys. Plasmas* **9**, 3617 (2002).
 - [7] A.A. Balakin, G.M. Fraiman, N.J. Fisch, and V.M. Malkin, *Phys. Plasmas* **10**, 4856 (2003).
 - [8] G.L. Lamb, Jr., *Phys. Lett.* **29A**, 507 (1969); *Rev. Mod. Phys.* **43**, 99 (1971); *Elements of Solution Theory* (Wiley, New York, 1980); V.E. Zakharov, *Pis'ma Zh. Éksp. Teor. Fiz.* **32**, 603 (1980) [*JETP Lett.* **32**, 589 (1980)]; S.V. Manakov, *ibid.* **35**, 193 (1982) [*ibid.* **35**, 237 (1982)]; V.A. Gorbunov, V.B. Ivanov, S.B. Papernyi, and V.R. Stratsev, *Izv. Akad. Nauk SSSR, Ser. Fez.* **48**, 1580 (1984) [*Bull. Acad. Sci. USSR Phys. Ser.* **48**, 120 (1984)]; J. Coste and C. Montes, *Phys. Rev. A* **34**, 3940 (1986).
 - [9] Yu.A. Tsidulko, V.M. Malkin, and N.J. Fisch, *Phys. Rev. Lett.* **88**, 235004 (2002).
 - [10] W. L. Kruer, *The Physics of Laser Plasma Interactions* (Addison-Wesley, Redwood City, CA, 1988), Chap. 7.
 - [11] D.L. Bobroff and H.A. Haus, *J. Appl. Phys.* **38**, 390 (1967).